Superconductivity, Susceptibility, and Specific Heat in the Noble Transition Elements and Alloys. I. Experimental Results*

K. ANDRES
Bell Telephone Laboratories, Murray Hill, New Jersey
AND
M. A. JENSEN†
University of Pennsylvania, Philadelphia, Pennsylvania

(Received 9 May 1967; revised manuscript received 16 August 1967)

We present experimental results of a study of superconductivity and magnetic susceptibility in face-centered-cubic alloys of Ir with Ru, Rh, Pd, Re, Os, and Pt, mostly on the Ir-rich side. The results show that the filling up of the d band first depresses the superconducting transition temperature and then causes the susceptibility to increase rapidly. There is a correlation between these two experimental parameters in that metals with large (exchange enhanced) susceptibilities are not superconducting above our experimental limit (0.015°K). We predict that Pd will not superconduct even at 0°K and that superconductivity in Rh and Pt will occur far below 10^{-3} °K, if at all.

I. INTRODUCTION

SUPERCONDUCTIVITY is a very common phenomenon among the nonmagnetic transition metals.[1] The only nonsuperconducting nonmagnetic transition metals (in the temperature range above 0.015°K) are Sc, Y and Lu[2] at the beginning and Rh, Pt and Pd at the end of the series, as indicated in Fig. 1. This is at first sight surprising since it is just these transition elements which have the highest electronic specific-heat coefficients, an account which favors superconductivity for all the other transition elements (except U). According to the Bardeen, Cooper and Schrieffer[3] (BCS) theory of superconductivity and its recent modifications[4–6] one expects the transition temperature to depend exponentially on a coupling between electrons which involves the density of states at the Fermi surface and the strength of the interactions between electrons, both the electron–electron Coulomb interactions and the electron–phonon–electron interactions. This expectation seems to be confirmed in many transition metals (elements and alloys) in that the variation in T_c can be explained by a variation of $N_\gamma(0)$, the density of states as measured by the electronic specific heat, assuming the interaction strengths (phonon attraction and Coulomb pseudopotential repulsion) to remain unchanged.[7,8] From the point of view of this theory, the lack of superconductivity near Sc and Pd might then be caused by either a decrease in the phonon attraction or an increase in the Coulomb (pseudopotential) repulsion. On the other hand, it may be that still another mechanism is present in these metals, which is sufficiently strong to inhibit superconductivity. In order to try to distinguish between these different possibilities, it was decided to study the occurrence of superconductivity in both regions as a function of alloy concentration and to compare the behavior of T_c with other properties of these alloys.

Some results of the work on the scandium metals have already been reported.[8] The work reported here concerns the behavior of T_c in the palladium metals, primarily in fcc solid solutions of iridium with its neighboring elements (Ru, Os, Rh, Pd, Pt). We also report measurements of the magnetic susceptibility for some of these alloys. A brief account of some of this latter work has been reported previously.[9,10]

In Sec. II, we describe the apparatus and the sample preparation. In Sec. III, the results of the superconductivity and susceptibility measurements are presented. In Sec. IV a qualitative discussion of these results is given and the usefulness of the electron density (number of valence electrons per cc) instead of the valence electron per atom ratio as a convenient parameter to describe the properties of the Pd metals is pointed out. In Sec. V we state the conclusions which can be drawn from this work. In the following article (hereafter called J-A) we analyze our results in terms of the BCS theory and in particular in terms of the recent theory by Berk and Schrieffer[5] about the effect

* Part of this work was carried out at the University of California at La Jolla and was supported, in part, by the U.S. Air Force Office of Scientific Research.

† Present address: University of Pennsylvania, Philadelphia, Pa. The work reported here which was carried out at La Jolla was taken from the thesis of M.A.J.

[1] B. T. Matthias, Phys. Rev. **97**, 74 (1955).

[2] We place Lu instead of La next to Hf in the periodic system, following D. C. Hamilton, Am. J. Phys. **33**, 637 (1965).

[3] J. Bardeen, L. N. Cooper, and J. R. Schrieffer, Phys. Rev. **108**, 1175 (1957).

[4] P. Morel and P. W. Anderson, Phys. Rev. **125**, 1263 (1962).

[5] N. F. Berk and J. R. Schrieffer, Phys. Rev. Letters **17**, 433 (1966).

[6] See for example, J. R. Schrieffer, *Theory of Superconductivity* (W. A. Benjamin, Inc., New York, 1964), and references cited therein.

[7] M. A. Jensen, Ph.D. thesis, University of California, La Jolla, 1966 (unpublished).

[8] M. A. Jensen and J. P. Maita, Phys. Rev. **149**, 409 (1966).

[9] M. A. Jensen, B. T. Matthias, and K. Andres, Science **150**, 1448 (1966).

[10] Paper given at the 10th Magnetism Conference in Washington, 1966 (unpublished).

Sc	Ti 0.39	V 5.37					
Y	Zr 0.52	Nb 9.36	Mo 0.91	Tc 7.92	Ru 0.49	Rh	Pd
Lu	Hf 0.095	Ta 4.48	W 0.012	Re 1.70	Os 0.66	Ir 0.11	Pt

FIG. 1. Occurrence of superconductivity in the nonmagnetic transition metals at temperatures above 10^{-2} °K. The figures denote the transition temperature.

of ferromagnetic spin fluctuations on superconductivity and on the electronic specific heat.[11]

II. EXPERIMENTAL

A. Apparatus

The work described here was carried out simultaneously at the Bell Telephone Laboratories in Murray Hill, New Jersey and at the University of California in La Jolla. In both places, an adiabatic demagnetization cryostat was used to cool the samples. The details of those cryostats will be published elsewhere. Only brief descriptions are given below.

The cryostat at Bell Laboratories has an outer helium Dewar which contains a movable superconducting solenoid of 9-in. length and 3-in. bore capable of producing 25 kG. The inner Dewar fits into the coil bore and contains the sample chamber. The cooling salt pill consists of a mixture of equal volumes of powdered $CrK(SO_4)_2 \cdot 12H_2O$ and epoxy resin (Hysol) and about 500 No. 42 Formex coated copper wires. The copper wires form a 13-in. long bundle below the salt pill which itself is supported by means of a nylon tube in the vacuum can. A movable Permendur shield around the vacuum can reduce the earth's magnetic field to about 10^{-2} Oe. Samples are soaked in Apiezon grease and stuck into these Cu wires. Superconductivity is detected by measuring the ac susceptibility of the samples at 25 or 80 cps. Mutual inductance coils are wound on the tail of the tail-shaped vacuum can, and the transitions are displayed on a recorder which measures the zero offset of a Hartshorn mutual inductance bridge. The temperature is measured by a heavily As-doped germanium resistor which is also stuck into the copper wires. This resistor in turn has been calibrated against the susceptibility of a cerium magnesium nitrate single crystal.[12] Helium gas is used to cool the cooling pill to 1.2°K. A demagnetization from 25 000 G leads to a final temperature of $\sim 0.013 \pm 0.002$°K. In order to improve the thermal insulation after demagnetization, the cooling salt and the samples are surrounded by a guard shield which itself is cooled by the same demagnetization to about 0.2°K. While the heat leak into the guard shield is of the order of 100 ergs/min, the residual heat leak into the samples and the cooling salt remains as low as a few ergs/min for about 1 h after demagnetization.

The cryostat at La Jolla has only one helium-4 bath which is pumped to 1.1°K. A stationary superconducting solenoid 7 in. long with $1\frac{3}{8}$ in. bore and capable of producing 15 kG demagnetizes a cerium magnesium nitrate (CMN) cooling salt pill grown around copper wires from 0.3 to below 0.01°K. The 0.3°K starting temperature is obtained by use of a helium-3 evaporator which also cools a shield surrounding the salt and samples. The heat leak to the samples ($\sim$2 ergs/sec) keeps the samples from getting colder than 0.02°K. Five samples are placed inside mutual inductance coils which are themselves enclosed inside a slotted copper block. The samples are glued with G.E. 7031-Toluol to copper screws which screw into the block. Superconductivity is detected by measuring the ac susceptibility of the samples using a 0.01 G (peak to peak) 100 cps primary field and phase sensitive detection. The temperature is measured by monitoring the susceptibility of a cerium magnesium nitrate single crystal which is mounted in a sixth set of secondary coils. The sample chamber is shielded from the earth's field by Mu metal and from the large demagnetizing field by a superconducting tantalum shield.

The low-temperature scales of both cryostats were checked against each other by means of superconducting transition temperatures of Ir–Pt samples and were found to agree within experimental error.

B. Sample Preparation

The purity of the materials used was nominally 99.99%. The samples were prepared in an argon arc furnace. Special care was taken in order to prevent sample contamination during preparation. Some samples and also the raw materials were especially checked for iron, since it is known that iron exhibits a local magnetic moment in Pd and Pt which could depress the superconducting transition temperature if present in even very small concentrations. The iron content was found to be lower than 50 ppm in Ru, Os and Ir and less than 10 ppm in Rh, Pd, and Pt. Since the samples made in La Jolla and at Bell Laboratories were often made from starting elements obtained from different suppliers, the consistency of the results gives a good deal of confidence that there are no major impurity problems.

The sample size varied between 5 and 20 mm^3. It was generally observed that the smaller samples had somewhat sharper superconducting transitions, indicating better homogeneity.

[11] N. F. Berk, Ph.D. thesis, University of Pennsylvania, 1966 (unpublished).

[12] The thermal equilibrium time between the crystal and the copper wires gets to be rather long below 0.020°K ($\sim\frac{1}{2}$ h), so that temperatures below 0.020°K were usually determined by extrapolating the Ge-resistor characteristic.

TABLE I. Superconducting transition temperature T_c, valence electron per atom ratio and some specific-heat data (γ=electronic specific-heat coefficient, Θ_D=Debye temperature) of Ir-rich binary alloys with Re, Os, Pt, Mo, W, V, Nb, and Ta. Alloys designated by equal numbers in front have the same valence electron per atom ratio, the same percentage of 4*d* atoms and similar transition temperatures.

Alloy (nominal atomic fractions)	T_c (°K)	Electrons per atom	γ 10^{-4} cal/°K² mole	Θ_D (°K)
Ir	0.10–0.11	9.00		
$Ir_{0.95}Re_{0.02}$	0.109–0.112	8.92		
$Ir_{0.96}Re_{0.04}$	0.130–0.142	8.92		
$Ir_{0.93}Re_{0.07}$	0.197–0.220	8.86		
$Ir_{0.9}Re_{0.1}$	0.28–0.34	8.80		
7, $Ir_{0.55}Re_{0.15}$	0.445–0.61	8.70		
8, $Ir_{0.80}Re_{0.20}$	0.66	8.6		
$Ir_{0.7}Re_{0.30}$	1.4–1.7	8.4		
$Ir_{0.75}Os_{0.25}$	0.37–0.40	8.75		
7, $Ir_{0.7}Os_{0.3}$	0.40–0.48	8.7	6.82	410
8, $Ir_{0.6}Os_{0.4}$	0.73	8.6		
$Ir_{0.9}Pt_{0.1}$	0.053–0.066	9.1		
$Ir_{0.8}Pt_{0.2}$	0.032–0.046	9.2		
$Ir_{0.987}Mo_{0.013}$	0.105–0.107	8.96		
$Ir_{0.973}Mo_{0.027}$	0.125–0.133	8.92		
$Ir_{0.953}Mo_{0.047}$	0.156–0.168	8.86		
$Ir_{0.9}Mo_{0.1}$	0.29	8.7	5.0	470
$Ir_{0.82}Mo_{0.18}$	0.44–0.50	8.46		
$Ir_{0.987}W_{0.013}$	0.105–0.107	8.96		
$Ir_{0.973}W_{0.027}$	0.123–0.125	8.92		
$Ir_{0.953}W_{0.047}$	0.147–0.162	8.86		
$Ir_{0.9}W_{0.1}$	0.20–0.23	8.7	6.1	417
$Ir_{0.85}W_{0.15}$	0.25–0.41	8.55		
$Ir_{0.99}V_{0.01}$	0.086–0.11	8.86		
$Ir_{0.98}V_{0.02}$	0.082–0.115	8.92		
$Ir_{0.965}V_{0.035}$	0.135–0.147	8.86		
$Ir_{0.85}V_{0.15}$	0.123–0.26	8.4		
$Ir_{0.99}Nb_{0.01}$	0.084–0.102	8.96		
$Ir_{0.98}Nb_{0.02}$	0.082–0.115	8.92		
$Ir_{0.965}Nb_{0.035}$	0.11–0.138	8.86		
$Ir_{0.925}Nb_{0.075}$	0.16–0.172	8.70	6.50	416
$Ir_{0.9}Nb_{0.1}$	0.049–0.060	8.60		
$Ir_{0.99}Ta_{0.01}$	0.096–0.116	8.96		
$Ir_{0.98}Ta_{0.03}$	0.127	8.88		
$Ir_{0.94}Ta_{0.06}$	0.150	8.76		
$Ir_{0.925}Ta_{0.075}$	0.11–0.125	8.70	6.13	408
$Ir_{0.9}Ta_{0.1}$[a]	0.050–0.067	8.60		
$Ir_{0.85}Ta_{0.15}$[a]	<0.024	8.40		

[a] These alloys were x rayed and found to be face-centered cubic.

III. RESULTS

A. Binary Alloys among 5*d*-Elements: Re–Ir, Os–Ir, and Pt–Ir

The transition temperatures observed for alloys among these series are summarized in Table I. In Fig. 2(a), we plot the log of T_c for these alloys versus their valence electron per atom ratio. The bars indicate the width of the transitions. It can be seen that to a good approximation the transition temperature is an exponential function of the electron per atom ratio. The fact that the Re and Os alloys fall on the same line on this plot suggests the validity of a rigid-band approximation. As soon as the valence difference between the solute atoms and the solvent Ir exceeds 2, however, this approximation breaks down. This is shown by the broken lines in Fig. 2(b) which indicate the variation in transition temperature with the electrons per atom

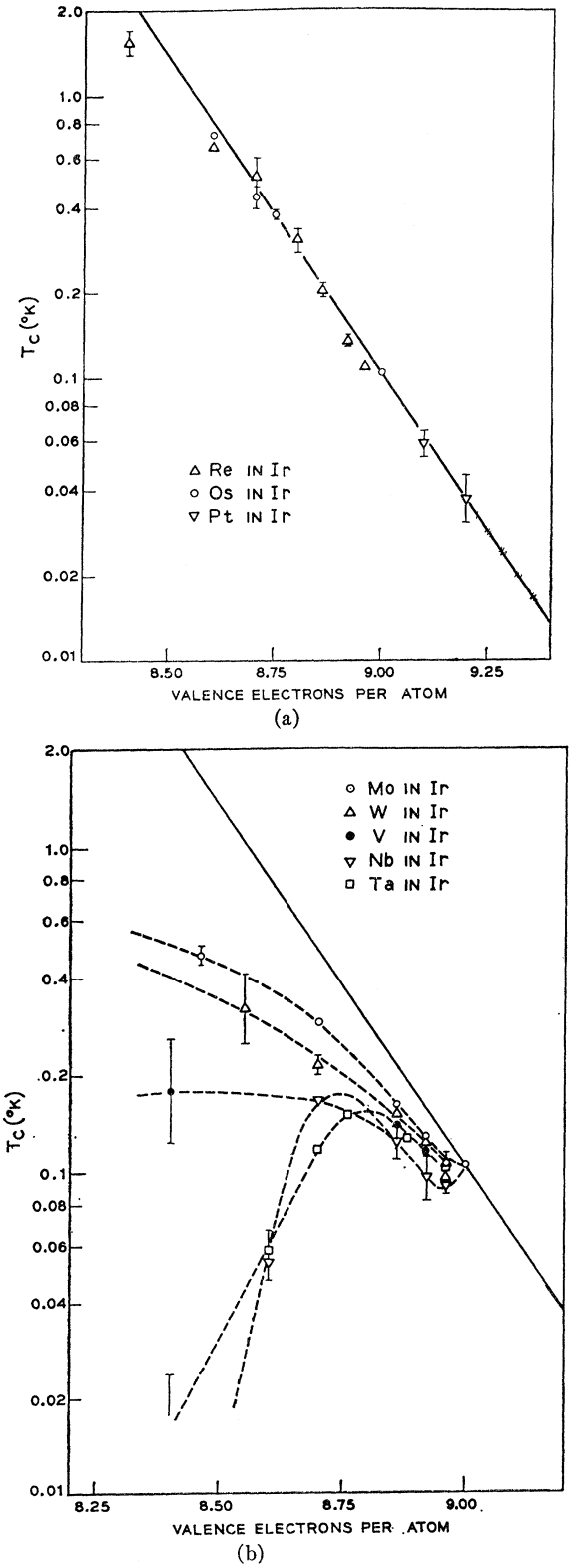

FIG. 2. (a) The variation of the superconducting transition temperature with the valence electron per atom ratio in face-centered-cubic Re–Ir, Os–Ir and Pt–Ir alloys. (b) The variation of the superconducting transition temperature with the valence electron per atom ratio in face-centered-cubic Mo–Ir, W–Ir, V–Ir, Nb–Ir, and Ta–Ir alloys.

ratio which we observed in fcc alloys of Mo and W, and of V, Nb and Ta in Ir. While the data of the Mo and W alloys could still be interpreted in terms of an effective valency difference between Mo and Ir, and W and Ir which would be about 2 and 1.5, respectively, instead of 3; the rapid disappearance of SC especially in the Ir–Ta and Ir–Nb alloys must be due to drastic changes in the electronic properties from that of pure Ir, brought about by the large nuclear charge difference between Nb or Ta and Ir. These changes do not seem to be significantly reflected in the electronic specific heat, since the alloys $Ir_{0.925}Nb_{0.075}$ and $Ir_{0.925}Ta_{0.075}$ have electronic specific heat coefficients very similar to the corresponding alloy $Ir_{0.7}Os_{0.3}$ (6.5 and 6.13, respectively, as compared to 6.7×10^{-4} cal/mol °K²). We therefore

TABLE II. Superconducting transition temperature T_c, valence electron per atom ratio and percentage of 4*d* atoms in Ir-rich binary alloys with Ru, Rh and Pd. See caption of Table III.

Alloy (nominal atomic fractions)	T_c (°K)	Electrons per atom	% 4*d*
$Ir_{0.925}Ru_{0.075}$	0.11	8.925	7.5
$Ir_{0.89}Ru_{0.11}$	0.105	8.89	11
$Ir_{0.845}Ru_{0.155}$	0.11	8.845	15.5
$Ir_{0.8}Ru_{0.2}$	0.13	8.8	20
$Ir_{0.765}Ru_{0.235}$	0.142	8.765	23.5
$Ir_{0.71}Ru_{0.29}$[a]	0.18	8.71	29
$Ir_{0.95}Rh_{0.05}$	0.055–0.075	9	5
$Ir_{0.89}Rh_{0.11}$	0.050–0.060	9	11
$Ir_{0.815}Rh_{0.185}$	0.028	9	18.5
$Ir_{0.80}Rh_{0.2}$	0.02–0.03	9	20
$Ir_{0.75}Rh_{0.25}$	0.020–0.026	9	25
$Ir_{0.7}Rh_{0.3}$	<0.014	9	30
$Ir_{0.96}Pd_{0.04}$	0.057–0.069	9.04	4
$Ir_{0.95}Pd_{0.05}$	0.035–0.050	9.05	5
$Ir_{0.91}Pd_{0.09}$	0.033–0.047	9.09	9
$Ir_{0.9}Pd_{0.1}$	0.032	9.1	10
$Ir_{0.88}Pd_{0.12}$	0.022–0.035	9.12	12

[a] This alloy was x rayed and found to be face-centered cubic.

conclude that it is mainly the effective electron–electron interaction rather than the density of states at the Fermi surface that decreases rapidly with increasing Nb and Ta concentration in these alloys.

B. Binary Alloys between 4*d* and 5*d*-Elements: Ir–Ru, Ir–Rh, and Ir–Pd

The results on fcc alloys from these systems are given in Table II and shown in Fig. 3 where we plot the log of the transition temperature against the atom percentage of Ru, Rh and Pd in Ir. The Ir–Rh system was originally investigated with the intention of extrapolating to a possible SC transition temperature of pure Rh. Such an extrapolation is, however, not very meaningful because the transition temperature of Ir–Rh alloys drops so fast with increasing Rh content. While the addition of Rh and Pt to Ir depresses the transition temperature equally fast, Pd is even more effective in depressing superconductivity.

TABLE III. Superconducting transition temperature T_c, valence electron per atom ratio and percentage 4*d* atoms in several Ir-rich ternary alloys with Ru, Rh, Pd, Re, Os, and Pt. Alloys designated by equal numbers in front (1 to 6) have the same valence electron per atom ratio, the same percentage of 4*d* atoms and similar transition temperatures.

Alloy (nominal atomic fractions)	T_c(°K)	Electrons per atom	% 4*d*
$(Ir_{0.8}Re_{0.2})$-Rh			
$Ir_{0.8}Re_{0.2}$	0.66	8.6	0
$(Ir_{0.8}Re_{0.2})_{0.9}Rh_{0.1}$	0.5–0.6	8.64	10
$(Ir_{0.8}Re_{0.2})_{0.8}Rh_{0.2}$	0.4–0.55	8.68	20
$(Ir_{0.8}Re_{0.2})_{0.7}Rh_{0.3}$	0.17–0.25	8.72	30
$(Ir_{0.8}Re_{0.2})_{0.575}Rh_{0.425}$	0.1–0.13	8.77	42.5
$(Ir_{0.8}Re_{0.2})_{0.5}Rh_{0.5}$	0.06–0.08	8.8	50
$(Ir_{0.7}Os_{0.3})$-Rh			
$Ir_{0.7}Os_{0.3}$	0.40–0.48	8.7	0
1, $(Ir_{0.7}Os_{0.3})_{0.9}Rh_{0.1}$	0.3–0.4	8.73	10
$(Ir_{0.7}Os_{0.3})_{0.8}Rh_{0.2}$	0.25–0.28	8.76	20
$(Ir_{0.7}Os_{0.3})_{0.7}Rh_{0.3}$	0.15–0.27	8.79	30
$(Ir_{0.7}Os_{0.3})_{0.58}Rh_{0.42}$	0.080–0.095	8.825	42
Ir–Os–Rh			
$Ir_{0.125}Os_{0.2}Rh_{0.675}$	0.03–0.05	8.8	67.5
$Ir_{0.54}Os_{0.1}Rh_{0.36}$	0.026–0.038	8.9	36
$Ir_{0.1}Os_{0.25}Rh_{0.65}$	0.07–0.10	8.75	65
5, $Ir_{0.6}Os_{0.1}Rh_{0.3}$	0.044–0.055	8.9	30
4, $Ir_{0.75}Os_{0.05}Rh_{0.2}$	0.047–0.055	8.95	20
$Ir_{0.1}Os_{0.3}Rh_{0.6}$	0.15–0.21°	8.7	60
$Ir_{0.55}Os_{0.15}Rh_{0.3}$	0.070–0.095	8.85	30
$Ir_{0.765}Os_{0.085}Rh_{0.15}$	0.075–0.096	8.916	15
3, $Ir_{0.6}Os_{0.20}Rh_{0.20}$	0.15–0.22	8.8	20
2, $Ir_{0.725}Os_{0.175}Rh_{0.1}$	0.13–0.16	8.825	10
$Ir_{0.125}Os_{0.375}Rh_{0.5}$[a,b]	0.3–0.46	8.625	50
$Ir_{0.4}Os_{0.3}Rh_{0.3}$	0.28–0.37		
$Ir_{0.18}Os_{0.47}Rh_{0.35}$[b]	0.48–0.55	8.53	35
6, $Ir_{0.1}Os_{0.2}Rh_{0.7}$[a]	<0.014	8.8	70
(IrRh)-Os			
$(IrRh)_{0.14}Os_{0.86}$	0.030–0.064	8.86	43
$(IrRh)_{0.175}Os_{0.825}$	0.080–0.095	8.825	41.5
$(IrRh)_{0.2}Os_{0.8}$	0.070–0.140	8.80	40
$(IrRh)_{0.27}Os_{0.73}$	0.20–0.22	8.73	36.5
$(IrRh)_{0.33}Os_{0.67}$	0.25–0.35	8.67	33.5
Ru-Ir-Rh			
$Ru_{0.3}Ir_{0.2}Rh_{0.5}$	0.045–0.055	8.7	80
$Ru_{0.25}Ir_{0.7}Rh_{0.5}$	0.028–0.033	8.75	75
5, $Ru_{0.1}Ir_{0.7}Rh_{0.2}$	0.04–0.05	8.9	30
4, $Ru_{0.05}Ir_{0.8}Rh_{0.15}$	0.064	8.95	20
6, $Ru_{0.2}Ir_{0.3}Rh_{0.5}$	0.01–0.02	8.8	70
Ir-Ru-Os			
2, $Ir_{0.825}Ru_{0.1}Os_{0.075}$	0.13–0.16	8.825	10
1, $Ir_{0.73}Ru_{0.1}Os_{0.17}$	0.31–0.34	8.73	10
Ir-Rh-Pt			
$Ir_{0.72}Rh_{0.20}Pt_{0.08}$	0.025–0.030	9.08	14
$Ir_{0.775}Rh_{0.05}Pt_{0.175}$	0.025–0.032	9.175	05
Ir-Pt-Pd			
$Ir_{0.83}Pt_{0.125}Pd_{0.045}$	0.030–0.037	9.17	4.5

[a] This alloy was x rayed and found to be face-centered cubic.

[b] These two alloys showed the presence of both face-centered cubic and hexagonal close packed.

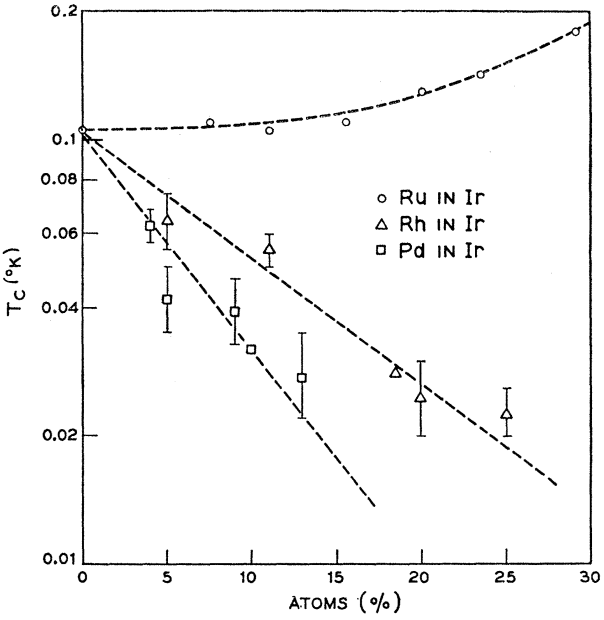

FIG. 3. The variation of the superconducting transition temperature with alloy concentration in face-centered-cubic alloys of Ru, Rh, and Pd in Ir.

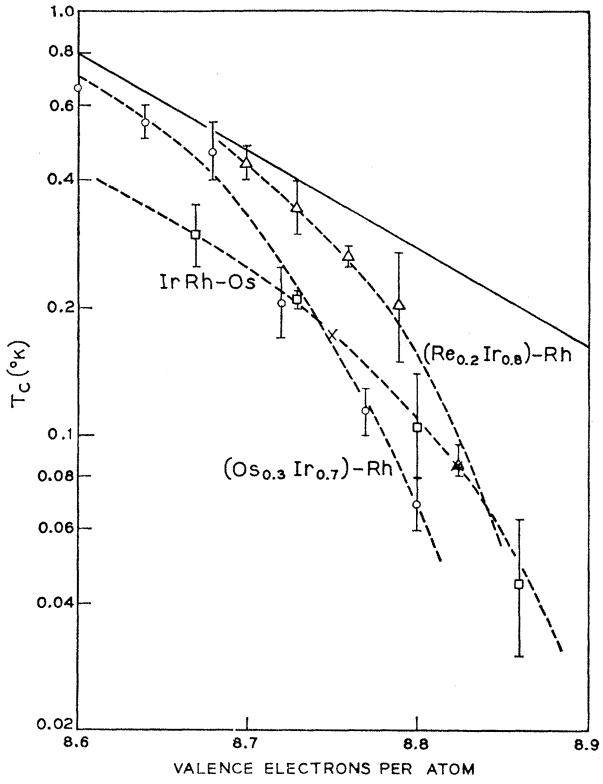

FIG. 4. The variation of the superconducting transition temperature with the valence electron per atom ratio in three ternary alloy series. The solid line indicates the T_c variation in the binary systems Os–Ir and Ir–Pt.

TABLE IV. Magnetic susceptibility χ, "susceptibility density of states" $n_\chi = \chi/2\mu_B^2$ (μ_B = Bohr magneton), valence electron per atom ratio, percentage 4*d* atoms and electron density n of Ir–Pd, Ir–Rh, Rh–Pd, Rh–Os alloys as well as of ternary alloys among Ru, Rh, Pd, Re, Os, Ir, and Pt. Alloys designated by equal numbers in front (1 to 4) have the same valence electron per atom ratio, the same percentage of 4*d* atoms, the same electron densities and similar susceptibilities.

Alloy (nominal atomic fractions)	χ (10^{-5} emu/mole)	n_χ (States/ eV atom)	Electrons per atom	% 4*d*	n (10^{23} electrons/cc)
$Ir_{0.1}Pd_{0.9}$	50.4	7.8	9.9	90	6.76
$Ir_{0.2}Pd_{0.8}$	20.9	3.24	9.8	80	6.71
$Ir_{0.3}Pd_{0.7}$	16.56	2.56	9.7	70	6.675
$Ir_{0.6}Pd_{0.4}$	8.51	1.32	9.4	40	6.54
$Ir_{0.88}Pd_{0.2}$	3.97	0.61	9.12	12	6.54
$Ir_{0.5}Rh_{0.5}$	6.25	0.97	9.0	50	6.45
$Ir_{0.75}Rh_{0.25}$	4.24	0.65	9.0	25	6.41
$Ir_{0.8}Rh_{0.2}$	3.48	0.55	9.0	20	6.40
$Ir_{0.9}Rh_{0.1}$	2.96	0.46	9.0	10	6.38
$Rh_{0.5}Pd_{0.5}$	24.7	3.83	9.5	100	6.67
$Rh_{0.25}Pd_{0.75}$	43.04	6.66	9.75	100	6.74
$Rh_{0.8}Pt_{0.2}$	12.74	1.97	9.2	80	6.55
$Rh_{0.8}Os_{0.2}$	7.46	1.15	8.8	80	6.38
$Ir_{0.4}Pd_{0.4}Rh_{0.2}$	13.2	2.05	9.4	60	6.57
$Ir_{0.25}Pd_{0.5}Rh_{0.25}$	17.22	2.67	9.5	75	6.63
$Ir_{0.5}Pd_{0.2}Rh_{0.3}$	7.77	1.21	9.2	50	6.50
$Ir_{0.1}Pd_{0.5}Rh_{0.4}$	21.9	3.39	9.5	90	6.65
$Ir_{0.2}Pd_{0.2}Rh_{0.6}$	11.75	1.82	9.2	80	6.55
$Ir_{0.54}Os_{0.1}Rh_{0.36}$	4.68	7.25	8.9	36	6.363
$Ir_{0.76}Os_{0.09}Rh_{0.15}$	2.98	0.46	8.91	15	6.36
$Ir_{0.6}Os_{0.1}Rh_{0.3}$	4.35	0.67	8.9	30	6.35
$Ir_{0.55}Os_{0.15}Rh_{0.3}$	4.21	0.65	8.85	30	6.32
$Ir_{0.75}Os_{0.05}Rh_{0.2}$	3.75	0.58	8.95	20	6.363
$Ir_{0.3}Rh_{0.5}Ru_{0.2}$	6.46	1.0	8.8	70	6.36
$Ir_{0.1}Os_{0.2}Rh_{0.7}$	6.25	0.97	8.8	70	6.36
$Ir_{0.3}Pt_{0.2}Rh_{0.5}$	9.21	1.44	9.2	50	6.50
$Pd_{0.25}Pt_{0.25}Rh_{0.5}$	21.4	3.32	9.5	75	6.63
$Pd_{0.4}Pt_{0.1}Rh_{0.5}$	23.5	3.64	9.5	90	6.65

C. Ternary Alloys among ReIrRh, OsIrRh, and RuIrRh

Ternary alloys were investigated for two reasons: First, in the hope of getting a better extrapolation to the transition temperature of Rh; and second, in order to check on the general validity of the apparent fact that solutes with 4*d*-electrons (Ru, Rh, and Pd) consistently lead to lower transition temperatures than solutes with 5*d* electrons (Os, Ir, and Pt). The results of all the ternary alloys investigated are given in Table III and are shown in Fig. 4. We find that within experimental error the transition temperature is only a function of the electron per atom ratio and the percentage of 4*d*-atoms in the alloy. In Fig. 5, we plot the transition temperature as a function of these two parameters, the x axis being the electron per atom ratio and the y axis measuring the percentage of 4*d*-atoms. Figure 5, thus, is a complete plot of SC in this section of the periodic system of the elements. Each point corresponds to an alloy of three elements forming the corners of a rectangular triangle in which the point is contained. Each point can, therefore, represent two alloys, since it lies in two such triangles unless it is located on a horizontal or vertical sideline and is therefore a binary alloy. The composition of each ternary alloy can be read off Fig. 5 in a manner which is explained in the figure caption. The solid lines are the approximate lines of constant transition temperature.

D. Magnetic Susceptibility of Binary and Ternary Alloys among Os, Ir, Rh, Pd, and Pt

The observed decrease in transition temperature with increasing electron concentration is followed by a substantial increase in magnetic susceptibility at higher electron concentrations. This has been shown previously in the alloy systems Rh–Pd and Ir–Pt.[13–15] In order to check whether the susceptibility, too, is only a function of the electron per atom ratio and the ratio of 4*d*- and 5*d*-atoms, we have measured the susceptibility of a number of binary and ternary alloys containing Os, Ir, Rh, Pd and Pt.[16] The results are given in Table IV. It can be seen that for alloys for which

[13] Again the values of the molar susceptibilities of 4*d* alloys are always higher than those for 5*d* alloys with the same number of valence electrons per atom.

[14] D. W. Budworth, F. E. Hoare, and J. Preston, Proc. Roy. Soc. (London) **257**, 250 (1960).

[15] T. H. Geballe *et al.*, J. Appl. Phys. **37**, 1181 (1966).

[16] These measurements were made with a balance method in 15 000 Oe and carried out by H. J. Williams and R. C. Sherwood at Bell Telephone Laboratories.

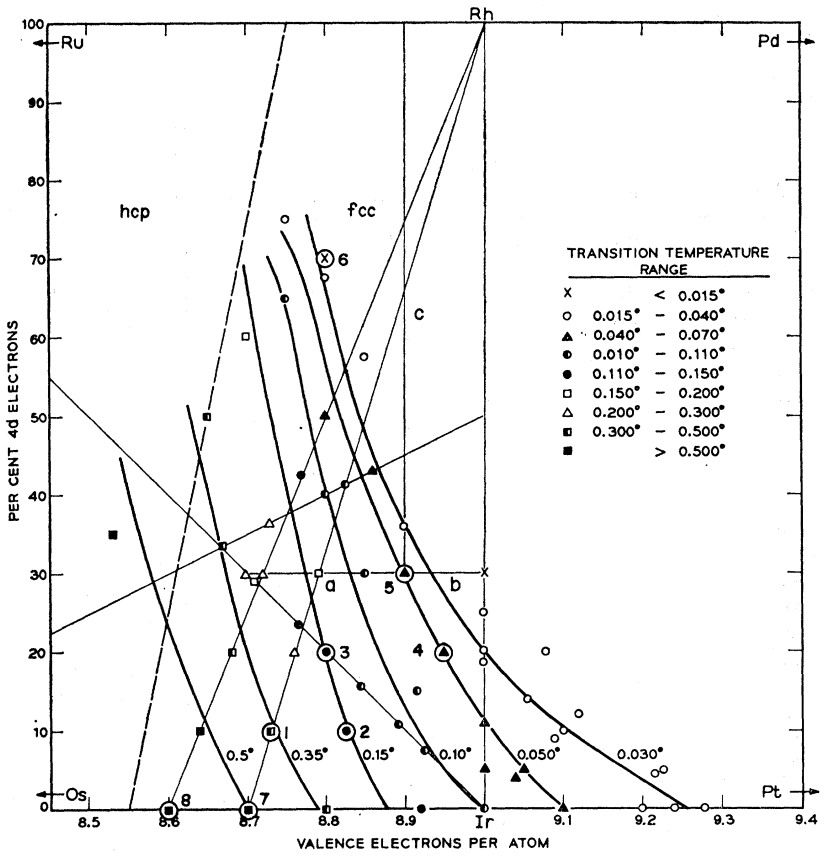

FIG. 5. Superconductivity in alloys of the noble transition metals Ru, Rh, Pd, and Os, Ir, Pt. Each point represents a binary or ternary alloy and is plotted according to its valence electron per atom ratio (x axis) and its percentage of $4d$ atoms (y axis). Each point lies in two rectangular triangles, the corners of which are three elements, and can, therefore, in general, represent two different ternary alloys. Point 5, for instance, can be the alloy $Ir_cRu_bRh_a$ or the alloy Ir_{c-b}, Os_b, Rh_{1-c} $(a+b+c=1)$. The numbered points surrounded by a circle actually represent two alloys, they are indicated by the same numbers in Tables II and III and have always very similar transition temperatures. The faint lines indicate alloy series. The labeled solid lines are the approximate lines of constant transition temperature.

TABLE V. Magnetic susceptibilities, "susceptibility density of states" n_χ (see Table IV for definition) and electron densities n of Pd–Pt, Pd–Rh, Ir–Pt, and Ir–Os alloys, taken from the literature.

Alloy	χ (10^{-6} emu/mole)	n_χ (states/eV atom)	n (10^{23} electrons/cc)	References and comments
Pd	78.0	12.1	6.790	at 20°K,[a]
$Pd_{0.9}Pt_{0.1}$	52.8	8.18	6.774	at 20°K,[a]
$Pd_{0.8}Pt_{0.2}$	39.5	6.12	6.758	at 20°K,[a]
$Pd_{0.6}Pt_{0.4}$	29.3	4.54	6.724	at 20°K,[a]
$Pd_{0.4}Pt_{0.6}$	28.5	4.41	6.691	at 20°K,[a]
$Pd_{0.2}Pt_{0.8}$	24.2	3.75	6.658	at 20°K,[a]
Pt	22.3	3.46	6.625	at 20°K,[a]
$PdRh_{0.0529}$	135	20.9	6.78	at 20°K,[b]
$Pd_{0.9073}Rh_{0.0927}$	109	16.9	6.77	at 20°K,[b]
$Pd_{0.8158}Rh_{0.1842}$	67.1	10.4	6.75	at 20°K,[b]
$Pd_{0.6512}Rh_{0.3488}$	38.2	5.92	6.72	at 20°K,[b]
$Pd_{0.4989}Rh_{0.5011}$	25.4	3.94	6.67	at 20°K,[b]
$Pd_{0.40}Rh_{0.60}$	20.0	3.10	6.645	at 20°K,[b]
$Pd_{0.246}Rh_{0.754}$	15.4	2.39	6.605	at 20°K,[b]
Rh	5.54	1.48	6.54	at 20°K,[b]
Pt	21.1	3.27	6.625	at 20°K,[b]
$Pt_{0.9488}Ir_{0.0512}$	21.9	3.40	6.61	at 20°K,[b]
$Pt_{0.902}Ir_{0.098}$	20.1	3.12	6.595	at 20°K,[b]
$Pt_{0.8013}Ir_{0.1987}$	15.4	2.39	6.58	at 20°K,[b]
$Pt_{0.6992}Ir_{0.3008}$	15.0	2.325	6.565	at 20°K,[b]
$Pt_{0.4998}Ir_{0.5002}$	8.08	1.25	6.50	at 20°K,[b]
$Pt_{0.313}Ir_{0.687}$	5.20	0.806	6.44	at 20°K,[b]
Ir	2.00	0.310	6.363	at 20°K,[b]
$Os_{0.10}Ir_{0.90}$	1.80	0.28	6.30	at 100°K,[a]
$Os_{0.30}Ir_{0.70}$	1.40	0.21	6.20	at 100°K,[a]
$Os_{0.40}Ir_{0.60}$	1.20	0.185	6.10	at 100°K,[a]

[a] Reference 15. [b] D. W. Budworth, F. E. Hoare, and J. Preston, Proc. Roy. Soc. (London) **257**, 250 (1960).

TABLE VI. Electronic specific heat γ "specific-heat density of states" $n_\gamma=3\gamma/2\pi^2k^2$ (k=Boltzmann's constant), Debye temperature Θ_D and electron density n of Pd–Rh, Os–Ir, and Ir–Pt alloys. Most of the data are taken from the literature.

Alloy	Specific heat γ (mJ/mole °K²)	n_γ (states/eV atom)	Θ_D (°K)	n (10^{23} electrons/cc)
Pd	9.31	1.96	274	6.79[a]
$PdRh_{0.0537}$	9.81	2.07	259	6.78[a]
$PdRh_{0.104}$	9.48	2.00	267	6.77[a]
$PdRh_{0.105}$	8.38	1.77	283	6.745[a]
$PdRh_{0.308}$	7.31	1.54	272	6.72[a]
$PdRh_{0.409}$	6.93	1.46	311	6.69[a]
$PdRh_{0.509}$	6.47	1.37	389	6.66[a]
Rh	4.65	0.98	512	6.54[a]
Os	2.35	0.50	500	5.720[b]
$Os_{35}Ir_{65}$	2.67	0.56	410	6.138[b]
$Os_{30}Ir_{70}$	2.85	0.60	410	6.171[b]
$Os_{10}Ir_{90}$	3.14	0.66	410	6.300[b]
Ir	3.27	0.69	425	6.363[b]
$Ir_{0.8}Pt_{0.2}$	3.42	0.72	377	6.415[b]
$Ir_{0.1}Pt_{0.9}$	6.45	1.36		6.599[c]
$Ir_{0.04}Pt_{0.96}$	6.59	1.39		6.615[c]
$Ir_{0.02}Pt_{0.98}$	6.68	1.41		6.620[c]
Pt	6.54	1.38	213	6.625[c]

[a] D. W. Budworth, F. E. Hoare, and J. Preston, Proc. Roy. Soc. (London) **257**, 250 (1960).
[b] Dixon *et al.*, in Proceedings of the Conference on the Electronic Structure of Alloys, Sheffield, 1963 (unpublished).
[c] J. P. Maita (private communication).

the values of these two parameters are the same, the susceptibility is indeed similar, which supports our expectation. The susceptibility and specific heat data for elements and binary alloys taken from the literature are given in Tables V and VI.

IV. DISCUSSION

A. Introductory Remarks

It was first shown by Matthias[1] that the superconducting transition temperature of transition elements and alloys is mainly a function of the average number of valence electrons per atom (number of valence electrons=all electrons outside the filled shell). We recall this empirical fact in Fig. 6 where we plot T_c versus the electron per atom ratio (e/a) for all nonmagnetic transition elements and a large number of alloys (data taken from the literature). We see that for all three rows ($3d$, $4d$ and $5d$) the behavior is very similar.

The Bardeen-Cooper-Schrieffer[3] (BCS) theory of superconductivity gives an expression for T_c which can be written approximately as

$$T_c \cong \Theta_D \exp\{-1/N(0)V_{\rm BCS}\}. \quad (1)$$

Θ_D is the Debye temperature, $N(0)$ the density of electronic states at the Fermi surface and $V_{\rm BCS}$ is a net attractive interaction between electrons. $V_{\rm BCS}$ in the original formulation of the theory was taken as the difference between the phonon-induced attraction and the Coulomb repulsion between electrons in the energy shell of width $2k\Theta_D$ centered at the Fermi surface. $N(0)$ was assumed to be proportional to γ, the linear term in the specific heat. Subsequently, the theory has been modified to properly consider both of these latter points. (See, for instance, Morel and Anderson,[4] Garland,[17] Schrieffer.[6]) From this modified theory [as is shown in J-A] one obtains an expression for T_c of the same form as Eq. (1), if we set

$$V_{\rm BCS}=(V_{\rm ph}-U_c)/[1+N(0)V_{\rm ph}], \quad (2)$$

where $N(0)$ is related to γ approximately by

$$N_\gamma(0)=3\gamma/2k^2\pi^2=N(0)[1+N(0)V_{\rm ph}]. \quad (3)$$

$V_{\rm ph}$ is the phonon attraction, U_c is called the Coulomb pseudopotential and k is Boltzmann's constant.[18] Since $N(0)V_{\rm ph}$ is probably less than 1 even for high-temperature superconductors, we expect from Eqs. (1), (2), and (3) that metals with large γ values should have higher transition temperatures, unless perhaps $V_{\rm ph}$ or U_c changes appreciably from metal to metal. In

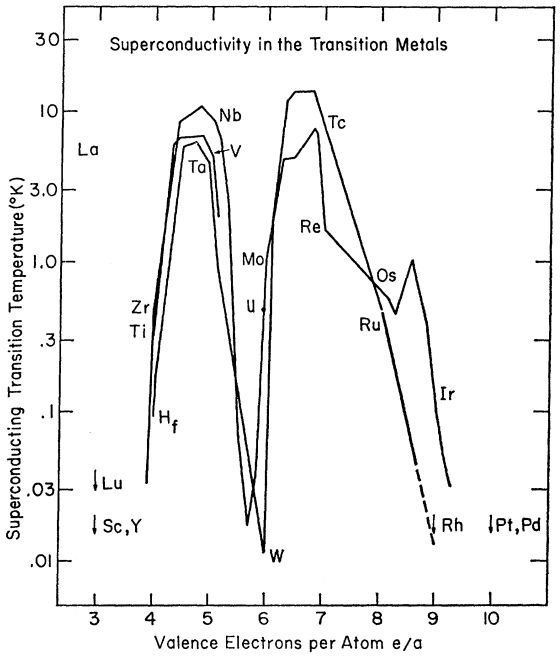

FIG. 6. The superconducting transition temperature in transition metals, plotted against the valence electron per atom ratio.

[17] J. W. Garland, Phys. Rev. Letters **11**, 111 (1963); Phys. Rev. **153**, 460 (1967).
[18] We call $N_\gamma(0)$ the "specific-heat density of states," which is enhanced over the "bare" density of states by electron–phonon and electron–electron interactions. Here we neglect the effect upon $N_\gamma(0)$ of Coulomb electron–electron interactions.

fact, if we study the variation of γ for the transition elements shown in Fig. 7 and compare this with the variation of T_c shown in Fig. 6, we see that in most cases this expectation is borne out. In particular, for $4\leq(e/a)\leq 8$ the variation of γ is qualitatively reflected in the behavior of T_c. However, the metals at the beginning $(e/a)\cong 3)$ and end $(e/a)\cong 10)$ of the transition series have very large γ values and still are not superconducting. Within the BCS theory there are a number of possible reasons for this: $V_{\rm ph}$ could be dropping off at the ends, U_c could be increasing, or an additional repulsive mechanism could be involved. One can attempt to distinguish between these possibilities by looking at the magnetic susceptibility. Also, there is reason to believe that the γ value is not always as simply related to $N(0)$ as indicated in Eq. (3); in particular, exchange interactions between the electrons may further renormalize their energies and enhance the quasiparticle density of states which one measures in the specific heat.

B. Transition Temperature, Susceptibility, Specific Heat and the Role of the Valence Electron Density

The Landau theory[19] predicts that Coulomb interactions between the electrons will enhance the spin susceptibility χ_p through the exchange interaction:

$$\chi_p/2\mu_B^2=N(0)/[1-N(0)\bar{V}_c]. \quad (4)$$

Here μ_B is the Bohr magneton and $\bar{V}_c$ is the difference between the Coulomb interaction for a pair of quasiparticles on the Fermi surface with parallel and antiparallel spin configurations. Dividing Eq. (4) by Eq. (3) yields

$$\frac{\chi_p/2\mu_B^2}{3\gamma/2k^2\pi^2}=\frac{N_\chi(0)}{N_\gamma(0)}$$
$$=[(1+N_0V_{\rm ph})(1-N_0\bar{V}_c)]^{-1}. \quad (5)$$

For Pd and Pt, χ_p is much larger than χ_v and χ_e, the Van Vleck paramagnetism and the Landau diamagnetism, respectively. For Rh, it is estimated from Knight shift data[20] that χ_v and χ_e just about cancel each other. We assume that the sum of χ_v and χ_e is small for Ir, too, and therefore take the total susceptibility χ to be a good measure of the spin susceptibility for these elements as well as for alloys between them. The ratio of Eq. (5) increases from around 1 for Ir to 2.4 for Pt and 5 for Pd, which means that $\bar{V}_c$ increases considerably as one moves from Ir to the right and up in the Periodic Table (see Fig. 1). It has been pointed out previously that the value of $N_0\bar{V}_c$ for Pd must be at least 0.9, close to the critical value of 1 for the ferromagnetic instability.[21]

As we pointed out in Sec. III, one of the main features of our results is that both T_c and χ (and also γ) depend predominantly on the number of valence electrons per atom and the ratio of $4d$ and $5d$ electrons. We show below that we are able to account for both these

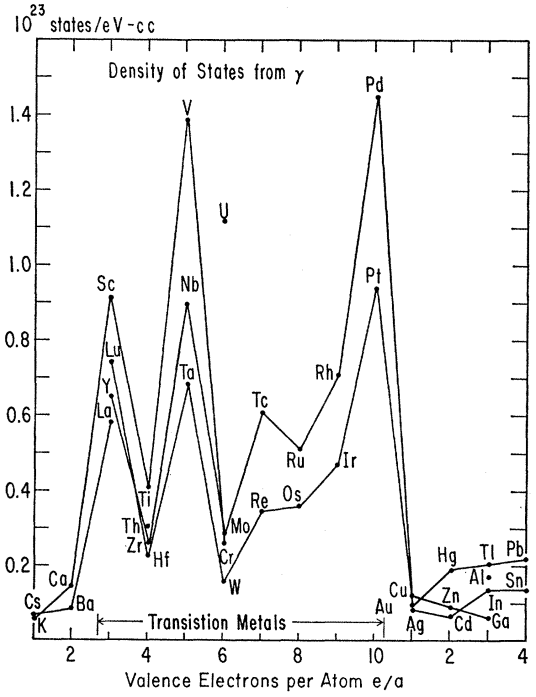

FIG. 7. The electronic specific heat of transition metals in units of states/eV cc [i.e., the "specific-heat density of states" $n_\gamma=(3\gamma/2k^2\pi^2)$] plotted against the number of valence electrons.

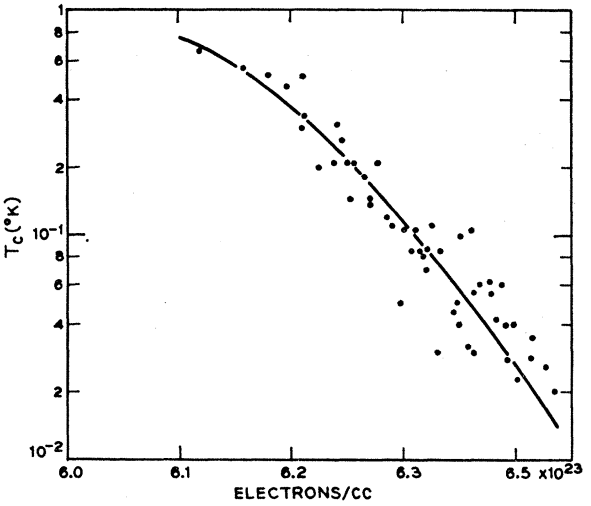

FIG. 8. The superconducting transition temperature of all the alloys investigated plotted against the valence electron density (valence electrons per cc).

[19] P. Nozieres, *The Theory of Interacting Fermi System* (W. A. Benjamin, Inc., New York, 1963).

[20] J. A. Seitchik, V. Jaccarino, and T. H. Wernick, Phys. Rev. **138**, A148 (1965).

[21] A. M. Clogston, V. Jaccarino, and Y. Yafet, Phys. Rev. **134**, A650 (1964).

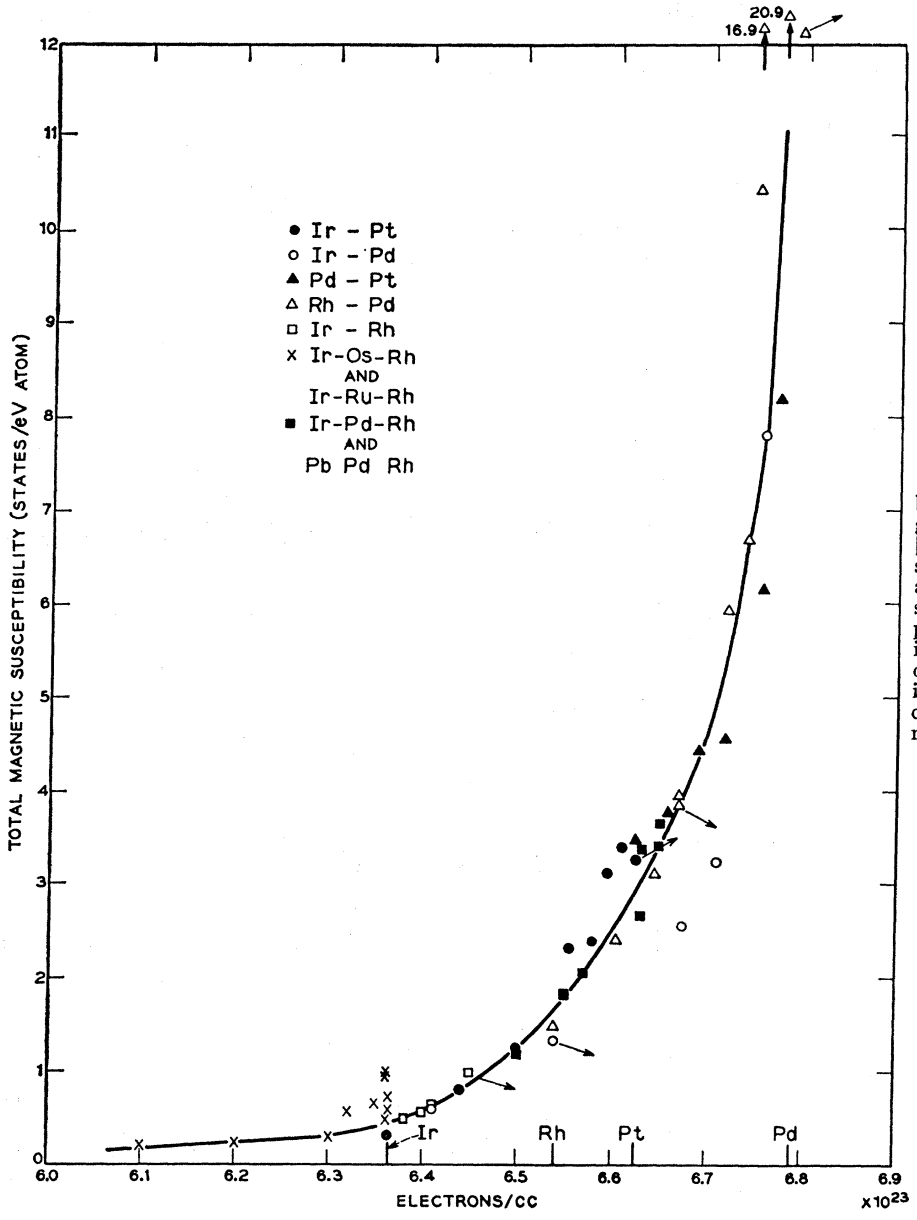

FIG. 9. The magnetic susceptibility of some of the alloys investigated, in units of states/eV atom [i.e. the "susceptibility density of states" $n_\chi=(\chi/2\mu_B^2)$], plotted against the valence electron density (number of valence electrons per cc). The arrows indicate the initial change in the susceptibility of some of the alloys upon an initial change of their volume, as computed from the observed magnetostriction.

dependencies by using a single parameter, the valence electron density n. In Figs. 8, 9, and 10, the T_c, χ, and γ data of all our alloys are plotted against this parameter, and it can be seen that we get reasonably uniform curves. Figure 11 is a summary of Figs. 8, 9, and 10 which shows a strong correlation between the rising susceptibility and the rapidly decreasing transition temperature. Unfortunately, T_c drops below our experimental limit of 0.015°K already when $N_\chi(0)\cong N_\gamma(0)$, i.e., when the susceptibility density of states equals the specific-heat density of states.

We offer the following qualitative explanation for the increase in the Coulomb repulsion with the electron per atom ratio and with the percentage of $4d$ atoms (i.e., with electron density). When the d band fills up with electrons, the Pauli principle causes the interaction between the ions to be more repulsive; therefore, the atomic volume increases. This leads to a more pronounced localization of the d-wave functions which might be expected to increase the intra-atomic Coulomb interaction. On the other hand, the observed increase in the Coulomb interaction with increasing $4d$-electron concentration for constant number of valence electrons per atom might be explained by the fact that the $4d$-wave functions themselves are more localized than the $5d$-wave functions. In going from a pure $5d$ to a pure $4d$ alloy at a constant electron per atom ratio, one changes the character of the d-electron wave function

from pure 5*d* to pure 4*d*. The intra-atomic Coulomb interactions thereby increase while the atomic volume decreases. It turns out experimentally that this volume decrease always amounts to about -2.7% for any electron per atom ratio between 8.5 and 10. If we assume the validity of Vegard's law,[22] then the lattice constant of an alloy varies linearly with the composition of its constituents; this then means that the mean atomic volume of our alloys is also only a function of the number of valence electrons per atom and the percentage 4*d* atoms (which is approximately equal to the percentage of 4*d* electrons).[23] One can thus increase the Coulomb interactions by either increasing the electron per atom ratio or the percentage of 4*d* electrons. On the other hand, one can also increase this latter percentage and at the same time decrease the electron per atom ratio so as to keep the Coulomb interaction constant. It turns out experimentally that this can be done if the two parameters are changed in such a way so as to keep the valence electron density (valence electrons per cc) constant. In other words, we can, to within a certain scatter, plot the T_c and χ data of all the alloys investigated as functions of the valence electron density only. Comparing Fig. 12 with Fig. 5

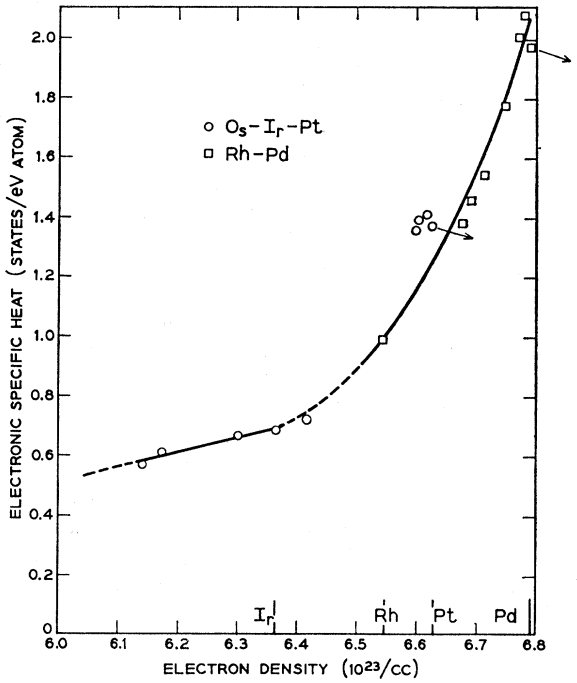

FIG. 10. The electronic specific heat of Os–Ir, Ir–Pt and Rh–Pd alloys, in units of states/eV atom, plotted against the valence electron density (number of valence electrons per cc). The arrows indicate the initial change in the electronic specific heat of Pt and Pd upon an initial change in atomic volume, as computed from thermal expansion data.

[22] L. Vegard, Z. Physik 5, 17 (1921).

[23] Such a plot of the mean atomic volume is shown in Fig. 12 which is reproduced from an earlier publication (See Ref. 9).

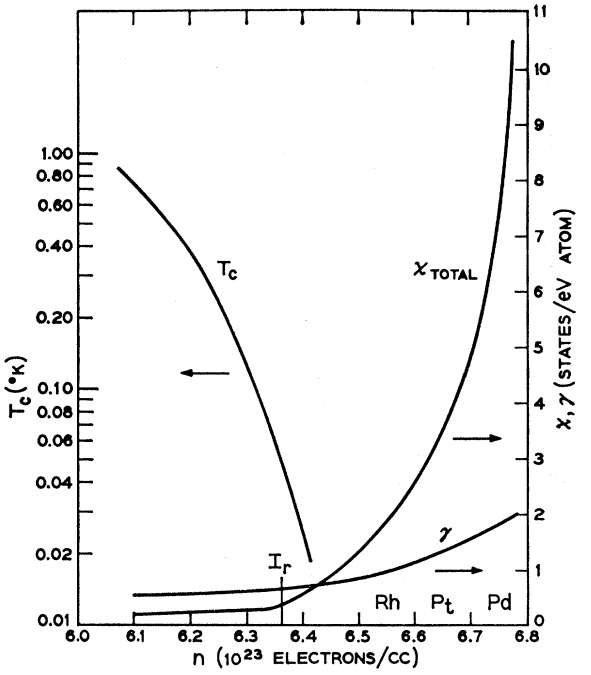

FIG. 11. The general trend of the superconducting transition temperature, the magnetic susceptibility and the electronic specfic heat as a function of the valence electron density of all the alloys investigated with electron densities higher than that of Re.

illustrates this fact in that lines of constant transition temperature are pretty much also lines of constant valence electron density.

We do not necessarily ascribe any specific physical significance to the electron density as a parameter, we merely use it as a convenient parameter in comparing the T_c, χ and γ data of a large number of alloys in order to study their relation. It should be pointed out that changing the electron density by increasing the number of electrons and changing it by changing the volume (i.e., by compressing the sample) does not always have the same effect on χ. This has been shown indirectly for some of our samples by measurements of their magnetostriction[24] and thermal expansion,[25] from which values for $\partial \ln\chi/\partial \ln V$ and $\partial \ln\gamma/\partial \ln V$ can be deduced. The initial changes of χ with electron density computed from those experiments are shown by arrows in Fig. 9. As can be seen, they do not always have the slope of the corresponding solid line. Thus, we are led to conclude that the electron density is apparently not an intrinsically important parameter.

C. Conclusions

Our results are summarized in Fig. 11. They are consistent with the assumption that the rapid drop

[24] We thank E. Fawcett (BTL) for prepublication use of these data.

[25] J. G. Collins and G. K. White, in *Progress in Low Temperature Physics*, edited by C. J. Gorter (Interscience Publishers Inc., New York, 1964), Vol. 4, p. 465.

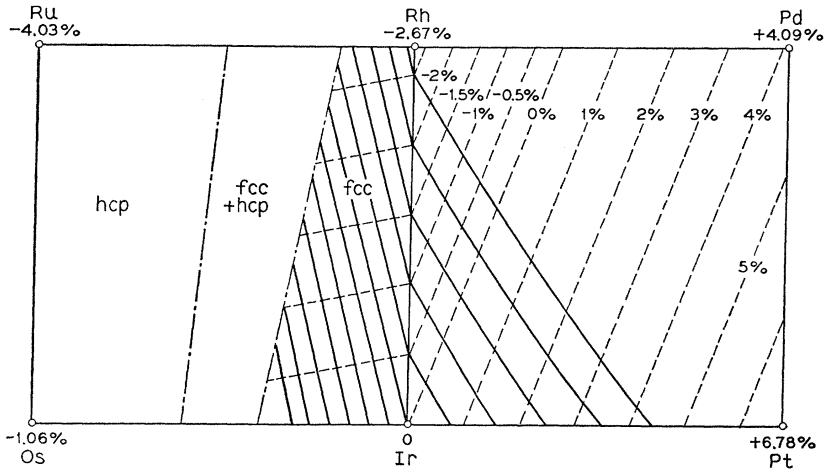

FIG. 12. Variation of atomic volume and electron density in face-centered-cubic (fcc) noble-metal transition elements and alloys. We have computed the data assuming the validity of Vegard's law and using room temperature values of lattice constants. The broken lines are lines of constant atomic volume, measured in the percentage deviation from the atomic volume of Ir (1.4143×10^{-23} cm^{-3}). The solid lines are lines of constant electron density, plotted in steps of 0.5% deviation from the electron density of Ir

($6.363\times10^{+23}$ cm^{3}).

in the superconducting transition temperature is caused mainly by an increasing Coulomb interaction between the electrons which, at higher electron concentrations, greatly enhances the spin susceptibility. A quantitative treatment of the results is hampered by the fact that the interesting regions of the T_c and χ data do not quite overlap. It was first suggested by Clogston[21] that Pd would not superconduct because of the large Coulomb repulsion (as computed from the susceptibility) which overcomes the phonon mediated attraction. However, his theory made no distinction between the different ways the Coulomb interaction enters the pairing interaction and the spin susceptibility. A reasonable extrapolation of our T_c data in Fig. 10 is nevertheless consistent with his prediction and also suggests that superconductivity in Rh and Pd occurs below 10^{-3} °K, if at all. Doniach[26] showed that the large exchange interaction between the d electrons in Pd should give rise to local ferromagnetic spin fluctuations which could be sufficiently retarded so as to compete with the phonon mediated attraction. This idea has recently been more fully developed by Berk and Schrieffer[5,20,11,27] who suggest that a large short range Coulomb interaction will cause a system to develop local spin fluctuations which can very effectively inhibit superconductivity. In the following article (J-A) it is shown that their theory predicts that this dynamic effect should still be important in alloys which have a much less exchange enhanced susceptibility than Pd. These critical spin fluctuations can also greatly enhance the electronic specific heat, in addition to the enhancement caused by the electron-phonon interaction. In J-A the importance of the dynamic interactions between electrons caused by the exchange interaction is critically evaluated. While it is uncertain whether spin fluctuations are in fact important in the superconductors we have investigated, it seems likely that they are important in the Pt and Pd rich alloys and so may explain the fact that both χ and γ depend on the same parameter, electron density, which then must somehow properly gauge the exchange interaction in these metals.

[26] S. Doniach, in Proceedings of the Manchester Many-Body Conference, September, 1964 (unpublished).

[27] J. R. Schrieffer and N. F. Berk, in *Proceedings of the Tenth International Conference on Low-Temperature Physics, Moscow, 1966* (Proizvodstrenno-Izdatel'skii Kombinat, VINITI, Moscow, USSR, 1967); W. L. McMillan (to be published).

ACKNOWLEDGMENTS

We would like to thank H. L. Luo and E. Corenzwit for preparing some of the samples, H. J. Williams and R. C. Sherwood for susceptibility measurements, and J. P. Maita for specific-heat measurements on some of the samples. We are indebted to W. L. McMillan, T. H. Geballe, and B. T. Matthias for stimulating and illuminating discussions. One of us (M.A.J.) thanks J. M. Goodkind for technical advice on adiabatic demagnetization and T. F. Smith, R. A. Simpkins, S. B. Sears, R. E. Siemon, and B. R. Maple for help in building the apparatus.